

NUMERICAL STUDY OF THE FLOW AND HEAT TRANSFER IN A REINER–RIVLIN FLUID ON A ROTATING POROUS DISK

H. A. Attia

UDC 532

An unsteady flow and heat transfer to an infinite porous disk rotating in a Reiner–Rivlin non-Newtonian fluid are considered. The effect of the non-Newtonian fluid characteristics and injection (suction) through the disk surface on velocity and temperature distributions and heat transfer is considered. Numerical solutions are obtained over the entire range of the governing parameters.

Key words: *non-Newtonian fluid, porous disk, injection, suction.*

Introduction. Rotating disk flows have practical applications in many areas, such as rotating machinery, lubrication, oceanography, computer storage devices, viscometry, and crystal growth processes. The problems of the fluid flow generated by a rotating disk was first formulated by von Kármán in 1921 [1]. Cochran [2] obtained an asymptotic solution of the steady problem. Benton [3] improved the steady-state solution [2] and extended the problem to the transient state. Stuart introduced suction through the disk surface [4] and solved the equations with zero rotation at infinity. Ockendon [5] used asymptotic methods to determine the solution of the problem for small values of the suction parameter and in the case of rotation at infinity. The effect of uniform injection through the disk surface on parameters of the flow induced by the rotating disk was analyzed by Kuiken [6]. In all the above-mentioned studies, the fluid was assumed to be Newtonian. A steady flow of a non-Newtonian fluid due to a rotating disk with uniform suction was considered by Mithal [7]; the solutions obtained were valid for small values of the parameter that describes the non-Newtonian behavior. Srivastava [8] extended the problem to the case of the fluid flow between two disks, one of them rotating and the other at rest.

The problem of heat transfer from a rotating disk maintained at a constant temperature was first considered by Millsaps and Pohlhausen [9] for a variety of Prandtl numbers in the steady state. For gases, the effects of compressibility were examined by Ostrach and Thornton [10]. Sparrow and Gregg [11, 12] studied the steady-state heat transfer from a rotating disk maintained at a constant temperature to fluids at arbitrary Prandtl numbers. Later, many authors have studied the heat transfer in the vicinity of a rotating disk for different thermal conditions [13–17].

In the present work, an unsteady laminar flow of a viscous incompressible Reiner–Rivlin non-Newtonian fluid, generated by uniform rotation of an infinitely large disk, is studied with allowance for heat transfer. Uniform suction (or injection) is applied at the disk surface. The disk temperature instantaneously increases and is assumed to be constant after that. The governing nonlinear partial differential equations are integrated numerically with the use of finite differences. Starting the motion from rest leads to a discontinuity between the initial and boundary conditions, which results in numerical oscillations. These oscillations are eliminated by means of suitable coordinate transformations. The effect of uniform injection (suction) through the disk surface on the characteristics of the non-Newtonian fluid flow and heat transfer is discussed.

Basic Equations. We consider a disk lying in the plane $z = 0$. The space $z > 0$ is filled by a viscous incompressible non-Newtonian fluid. The motion is started instantaneously from rest to disk rotation with a constant angular velocity ω about the line $r = 0$; uniform injection (suction) through the disk surface is applied. The injection (suction) velocity is varied within wide limits.

King Saud University, Buraidah 81999, KSA; ah1113@yahoo.com. Translated from *Prikladnaya Mekhanika i Tekhnicheskaya Fizika*, Vol. 46, No. 1, pp. 85–95, January–February, 2005. Original article submitted November 12, 2003; revision submitted April 2, 2004.

The equations of unsteady motion are given by

$$\frac{\partial u}{\partial r} + \frac{u}{r} + \frac{\partial w}{\partial z} = 0, \quad (1)$$

$$\rho \left(\frac{\partial u}{\partial t} + u \frac{\partial u}{\partial r} + w \frac{\partial u}{\partial z} - \frac{v^2}{r} \right) = \frac{\partial \tau_r^r}{\partial r} + \frac{\partial \tau_r^z}{\partial z} + \frac{\tau_r^r - \tau_\varphi^\varphi}{r}, \quad (2)$$

$$\rho \left(\frac{\partial v}{\partial t} + u \frac{\partial v}{\partial r} + w \frac{\partial v}{\partial z} + \frac{uv}{r} \right) = \frac{\partial \tau_\varphi^r}{\partial r} + \frac{\partial \tau_\varphi^z}{\partial z} + 2 \frac{\tau_\varphi^r}{r}, \quad (3)$$

$$\rho \left(\frac{\partial w}{\partial t} + u \frac{\partial w}{\partial r} + w \frac{\partial w}{\partial z} \right) = \frac{\partial \tau_z^r}{\partial r} + \frac{\partial \tau_z^z}{\partial z} + \frac{\tau_z^r}{r}, \quad (4)$$

where u , v , and w are the velocity components in the r , φ , and z directions, respectively, t is the time, and ρ is the fluid density. The constitutive equation for the Reiner–Rivlin non-Newtonian fluid is given in [7, 8]:

$$\tau_j^i = 2\mu e_j^i + 2\mu_c e_k^i e_j^k - p\delta_j^i, \quad e_j^j = 0. \quad (5)$$

Here p is the pressure (which does not represent the thermodynamic pressure but an arbitrary scalar since $\rho = \text{const}$), τ_j^i is the stress tensor, e_j^i is the strain-rate tensor, μ is the viscosity, $\mu_c = \alpha(c + \sum \sum e_j^i e_j^i)/2$ is the coefficient of cross viscosity, $c = \text{const}$, and α is a sufficiently small parameter (constant). The Reiner–Rivlin model is comparatively simple, but it provides a somewhat intuitive prediction of flow parameters and heat-transfer performance of a viscoelastic fluid above a rotating disk.

The initial and boundary conditions for the dynamic problem are written as

$$t = 0: \quad u = 0, \quad v = 0, \quad w = w_0; \quad (6a)$$

$$z = 0: \quad u = 0, \quad v = r\omega, \quad w = w_0; \quad (6b)$$

$$z = \infty: \quad u = 0, \quad v = 0, \quad p = p_\infty. \quad (6c)$$

The initial conditions are described by Eq. (6a). Equation (6b) defines the no-slip condition of the flow on the surface; the velocity normal to the surface specifies mass injection or withdrawal. Conditions at infinity are defined by Eq. (6c).

We introduce the von Kármán variables [1, 7]

$$u = r\omega F, \quad v = r\omega G, \quad w = \sqrt{\omega\nu} H, \quad z = \sqrt{\nu/\omega} \zeta, \quad p - p_\infty = -\rho\nu\omega P,$$

where ζ is the dimensionless distance along the axis of revolution, F , G , H , and P are dimensionless functions of ζ and t , and $\nu = \mu/\rho$ is the kinematic viscosity of the fluid. Because of injection (suction), the vertical component of velocity H takes a constant (non-zero) value at $\zeta = 0$. With these definitions, Eqs. (1)–(6) take the following form:

$$\frac{\partial H}{\partial \zeta} + 2F = 0; \quad (7)$$

$$\frac{\partial F}{\partial t'} - \frac{\partial^2 F}{\partial \zeta^2} + H \frac{\partial F}{\partial \zeta} + F^2 - G^2 + \frac{1}{2} K \left(\left(\frac{\partial F}{\partial \zeta} \right)^2 + 3 \left(\frac{\partial G}{\partial \zeta} \right)^2 + 2F \frac{\partial^2 F}{\partial \zeta^2} \right) = 0; \quad (8)$$

$$\frac{\partial G}{\partial t'} - \frac{\partial^2 G}{\partial \zeta^2} + H \frac{\partial G}{\partial \zeta} + 2FG - K \left(\frac{\partial F}{\partial \zeta} \frac{\partial G}{\partial \zeta} - F \frac{\partial^2 G}{\partial \zeta^2} \right) = 0; \quad (9)$$

$$\frac{\partial H}{\partial t'} - \frac{\partial^2 H}{\partial \zeta^2} + H \frac{\partial H}{\partial \zeta} + \frac{7}{2} K \frac{\partial H}{\partial \zeta} \frac{\partial^2 H}{\partial \zeta^2} - \frac{dP}{d\zeta} = 0; \quad (10)$$

$$F(0, \zeta) = 0, \quad G(0, \zeta) = 0, \quad H(0, \zeta) = S; \quad (11a)$$

$$F(t, 0) = 0, \quad G(t, 0) = 1, \quad H(t, 0) = S; \quad (11b)$$

$$F(t, \infty) = 0, \quad G(t, \infty) = 0. \quad (11c)$$

Here $t' = t\omega$, $K = \mu_c\omega/\mu$ is a parameter that describes the non-Newtonian behavior, and $S = w_0/\sqrt{\omega\nu}$ is the uniform injection (suction) parameter, which is negative in the case of suction and positive in the case of injection.

The range of variation of model parameters was chosen on the basis of a large number of numerical experiments. It was found that the parameter K should lie in the range $K < 3$, which corresponds to the range of the injection parameter $-2 \leq S \leq 2$. System (7)–(9) with the boundary and initial conditions (11) yields three components of velocity. Equation (10) can be used to find the pressure distribution if necessary.

The difference in temperature between the disk surface and the ambient fluid is responsible for heat transfer. The energy equation with neglected dissipation terms takes the form [12]

$$\rho c_p \left(\frac{\partial T}{\partial t} + u \frac{\partial T}{\partial r} + w \frac{\partial T}{\partial z} \right) - k \frac{\partial^2 T}{\partial z^2} = 0, \quad (12)$$

where T is the temperature, c_p is the heat capacity at constant pressure, and k is the thermal conductivity.

The initial and boundary conditions for the thermal problem imply an instantaneous change in temperature of the disk surface T_w from the state at rest.

In terms of the dimensionless temperature $\theta = (T - T_\infty)/(T_w - T_\infty)$ and von Kármán variables, Eq. (12) takes the form

$$\frac{\partial \theta}{\partial t'} - \frac{1}{\text{Pr}} \frac{\partial^2 \theta}{\partial \zeta^2} + H \frac{\partial \theta}{\partial \zeta} = 0, \quad (13)$$

where $\text{Pr} = c_p\mu/k$ is the Prandtl number. The initial and boundary conditions in the dimensionless form are expressed as

$$\theta(0, \zeta) = 0, \quad \theta(t, 0) = 1, \quad \theta(t, \infty) = 0. \quad (14)$$

The heat flux from the disk to the fluid is determined by the Fourier law $q = -k(\partial T/\partial z)_w$, which acquires the following form in dimensionless variables:

$$q = -k(T_w - T_\infty) \sqrt{\frac{\omega}{\nu}} \frac{\partial \theta(t, 0)}{\partial \zeta}.$$

By introducing the Nusselt number $\text{Nu} = q\sqrt{\nu/\omega}/(k(T_w - T_\infty))$, we reduce the last expression to

$$\text{Nu} = -\frac{\partial \theta(t, 0)}{\partial \zeta}.$$

Since all significant velocity and temperature variations are confined to a limited region adjacent to the disk, we define the thicknesses of the corresponding layers with the use of integral quantities [8]. For the tangential direction, we introduce the displacement thickness

$$\delta_{\text{dis}} = \int_0^\infty G d\zeta.$$

As the scale of the thermal layer thickness, we use a quantity determined by the temperature excess (over the ambient temperature) [8]

$$\delta_\theta = \int_0^\infty \theta d\zeta.$$

Numerical Solution. The numerical solution for the nonlinear equations (7)–(9) with conditions (11) by the finite-difference method involves numerical oscillations caused by the discontinuity between the initial and boundary conditions [Eqs. (11a) and (11b)]. The same refers to the thermal problem [see Eq. (14)]. A solution for this numerical problem could be achieved by using proper coordinate transformations proposed by Ames [19]. Expressing Eqs. (7)–(9) and (13) in terms of the modified coordinate $\eta = \zeta/2\sqrt{t'}$, we obtain

$$\frac{\partial H}{\partial \eta} + 4\sqrt{t'} F = 0; \quad (15)$$

$$\frac{\partial F}{\partial t'} - \frac{\eta}{2t'} \frac{\partial F}{\partial \eta} - \frac{1}{4t'} \frac{\partial^2 F}{\partial \eta^2} + \frac{1}{2\sqrt{t'}} H \frac{\partial F}{\partial \eta} + F^2 - G^2 + \frac{K}{8t'} \left(\left(\frac{\partial F}{\partial \eta} \right)^2 + 3 \left(\frac{\partial G}{\partial \eta} \right)^2 + 2F \frac{\partial^2 F}{\partial \eta^2} \right) = 0; \quad (16)$$

$$\frac{\partial G}{\partial t'} - \frac{\eta}{2t'} \frac{\partial G}{\partial \eta} - \frac{1}{4t'} \frac{\partial^2 G}{\partial \eta^2} + \frac{1}{2\sqrt{t'}} H \frac{\partial G}{\partial \eta} + 2FG - \frac{K}{4t'} \left(\frac{\partial F}{\partial \eta} \frac{\partial G}{\partial \eta} - F \frac{\partial^2 G}{\partial \eta^2} \right) = 0; \quad (17)$$

$$\frac{\partial \theta}{\partial t'} - \frac{\eta}{2t'} \frac{\partial \theta}{\partial \eta} - \frac{1}{4t'} \frac{1}{\text{Pr}} \frac{\partial^2 \theta}{\partial \eta^2} + \frac{1}{2\sqrt{t'}} H \frac{\partial \theta}{\partial \eta} = 0. \quad (18)$$

System (15)–(18) with conditions (11) and (14) was solved by the marching technique with the Crank–Nicholson implicit method [19]. The resulting system of differential equations was solved in an infinite domain $0 < \zeta < \infty$ and $0 < t' < \infty$. A finite domain in the ζ direction can be used instead, if ζ is chosen large enough to ensure that the solution is not affected by asymptotic conditions imposed at finite distances. Because of the coordinate transformation introduced in this work, however, this finite domain decreases with time and affects the accuracy of the numerical solution. To solve this problem, Eqs. (15)–(17) were integrated from $t' = 0$ to $t' = 1$. Then, the solution obtained at $t' = 1$ was used as the initial condition for integrating Eqs. (7)–(9) and (13) from $t' = 1$ toward the steady state.

Results and Discussion. Figure 1 shows the time-dependent growth of the axial velocity component at infinity H_∞ for different values of K and the injection parameter. Increasing K decreases the axial flow toward the disk, whereas the time needed to obtain a steady flow increases for all values of S . The effect of K on the steady-state time of H_∞ is more pronounced in the case of suction. Figure 1c indicates that the values of H_∞ in the case of injection change from positive to negative, and the time of this crossover increases with increasing parameter K . Figure 1b illustrates an interesting effect of reversing the flow direction with time for all values of K and $S = 0$. In fact, as is shown in Fig. 1a, the parameter H_∞ becomes positive for a certain time even in the case of suction for large values of K ($K = 2$). This means that the parameter K has an injection effect. It is also shown in Fig. 1 that the inclusion of the parameter K into consideration causes an overshooting in H_∞ . The amount of this overshooting in H_∞ over the steady value and the time of at which it occurs increase with increasing K .

Figure 2 shows the time-dependent growth of the tangential displacement thickness δ_{dis} for different values of K and the injection parameter S . Increasing K increases δ_{dis} and its steady-state time for all values of S . It is also shown that an increase in S increases δ_{dis} for all values of K . All curves in Fig. 2a and b are characterized by an overshooting, which increases with increasing K . In turn, in the case of suction, only high values of K ($K = 2$) yield an overshooting in the dependences $\delta_{\text{dis}}(t')$.

The time evolution of $\text{Nu}(t')$ for different K and S and for $\text{Pr} = 0.7$ is plotted in Fig. 3. Increasing K decreases the Nusselt number for all values of the injection parameter because an increase in K decreases the flow velocity toward the disk. The values of Nu are also significantly reduced with increasing injection parameter because there is a fluid layer with a temperature close to T_w near the disk surface. Suction has the opposite effect because the fluid whose temperature is close to the ambient temperature is brought to the neighborhood of the disk surface. It also follows from the results in Fig. 3 that the effect of the parameter K on the Nusselt number is more pronounced in the case of suction.

Figure 4 shows the dependence $\delta_\theta(t')$ for different K and S and the Prandtl number $\text{Pr} = 0.7$. Increasing K increases δ_θ because of the above-mentioned influence of this parameter on the fluid velocity toward the disk.

Figures 5–8 show the steady profiles of the parameters G , F , H , and θ , respectively, for different values of the injection parameter and $K = 0, 1$, and 2 . As is seen from Fig. 5, an increase in the parameters S and K leads to an increase in G for all values of ζ . The effect of suction velocity is more pronounced for higher values of K . In the case of injection, however, the dependence of the parameter $G(S)$ is more apparent for lower values of K . The calculation results plotted in Fig. 6 show that, in the case of injection (with $K = 0$), increasing S slightly decreases F for small values of ζ but significantly increases this parameter for large values of ζ . For $K \neq 0$ (see Fig. 6b and c), however, the values of F increase within the entire range with increasing injection velocity.

The data in Fig. 6a indicate that the parameter F decreases for all values of ζ with increasing suction velocity and $K = 0$. In the case $K \neq 0$ (Fig. 6b and c), however, an interesting effect is observed: the radial flow in the case of suction reverses its direction for all ζ , and the value of F increases with increasing K . The effect of suction velocity on the parameter F depends on ζ . As the suction velocity increases, the value of F increases for small values of ζ but decreases for large values of ζ .

This effect is observed in the case of suction and $K \neq 0$; it is manifested as a crossover of the curves $F(\zeta)$ corresponding to different values of S .

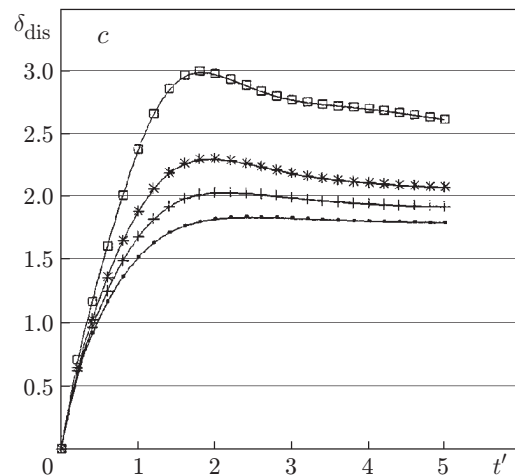
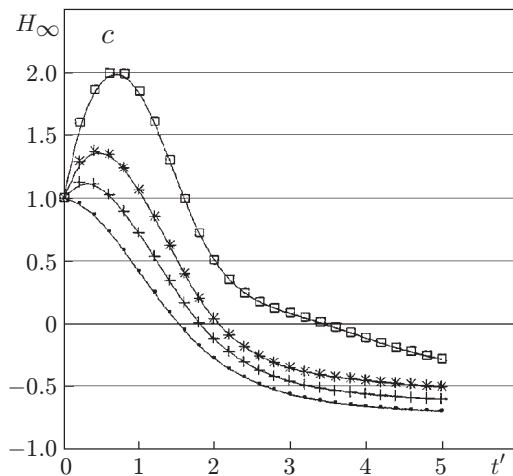
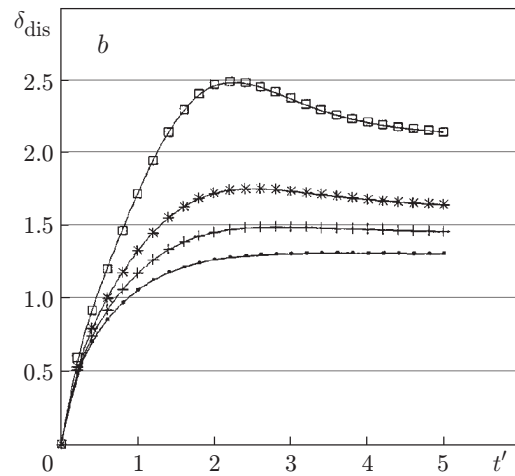
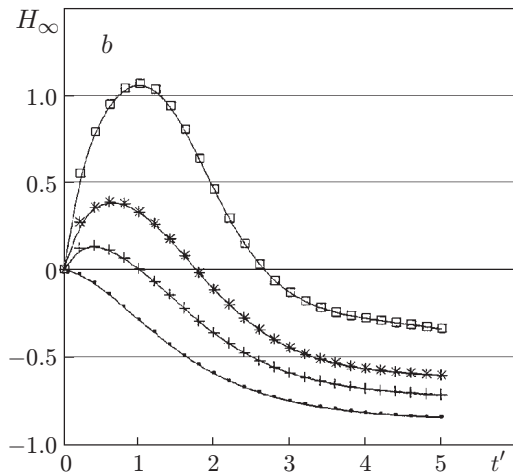
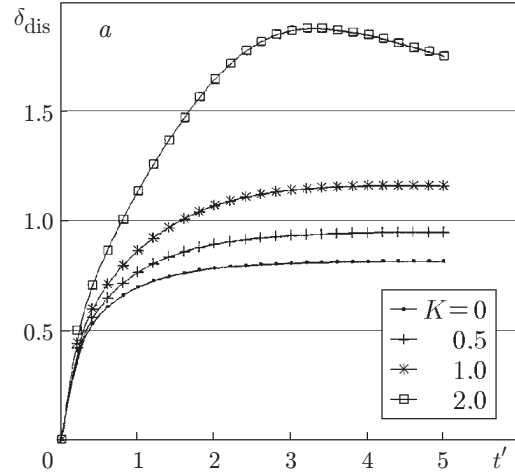
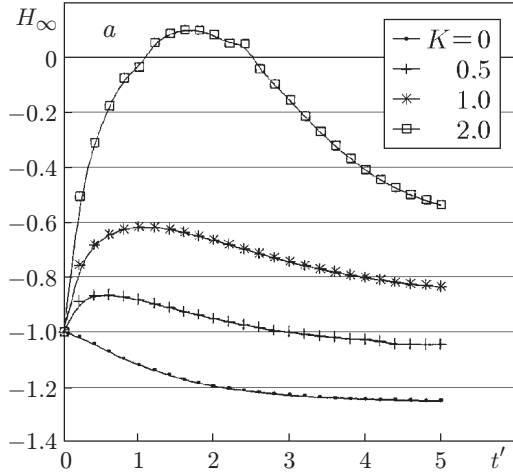


Fig. 1

Fig. 2

Fig. 1. Time evolution of the parameter H_∞ for different values of K and $S = -1$ (a), 0 (b), and 1 (c).

Fig. 2. Displacement thickness δ_{dis} versus time for different values of K and $S = -1$ (a), 0 (b), and 1 (c).

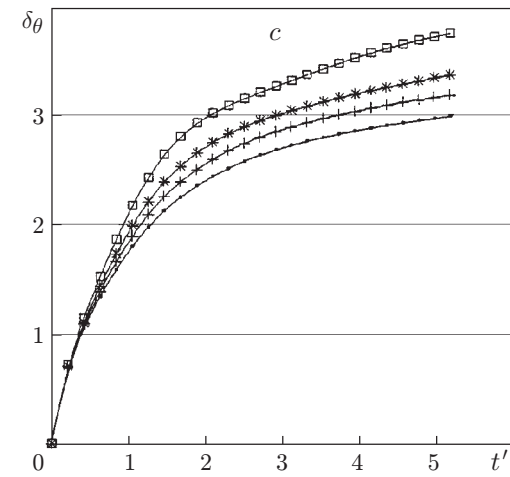
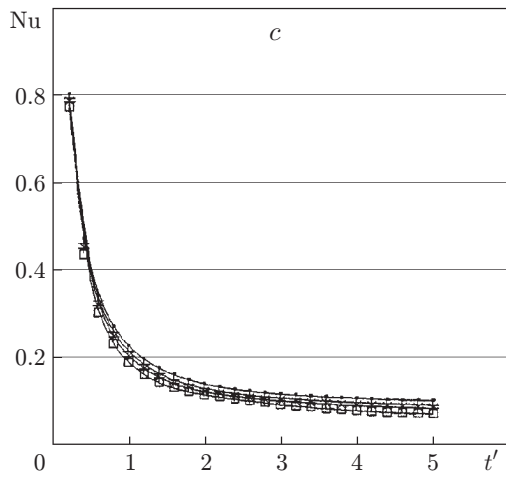
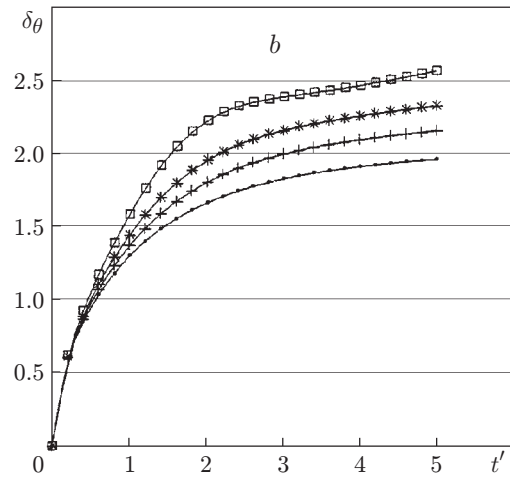
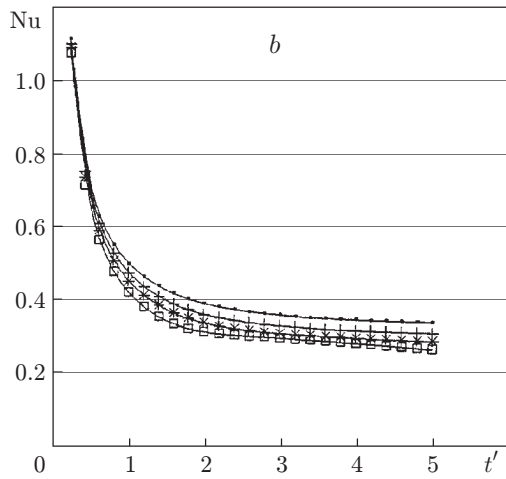
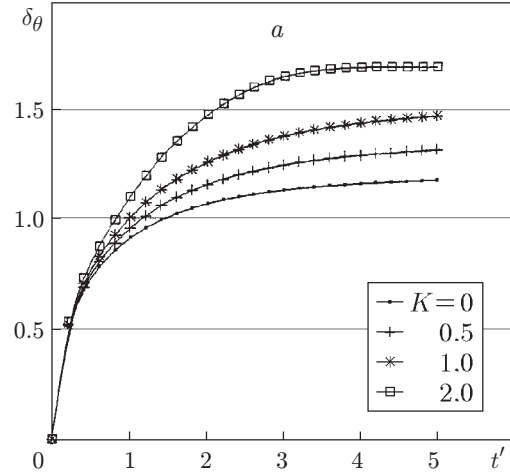
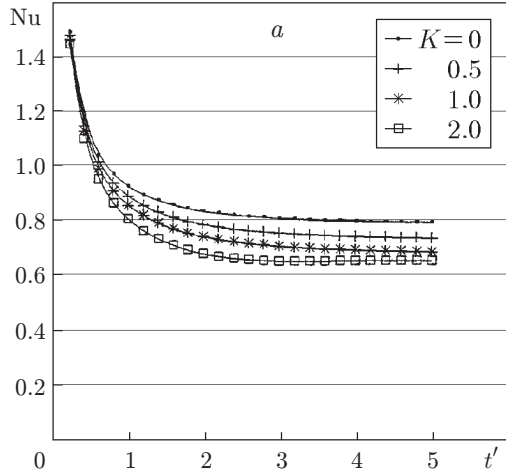


Fig. 3

Fig. 4

Fig. 3. Time evolution of the Nusselt number for different values of K and $S = -1$ (a), 0 (b), and 1 (c).

Fig. 4. Time evolution of the parameter δ_θ for different values of K and $S = -1$ (a), 0 (b), and 1 (c).

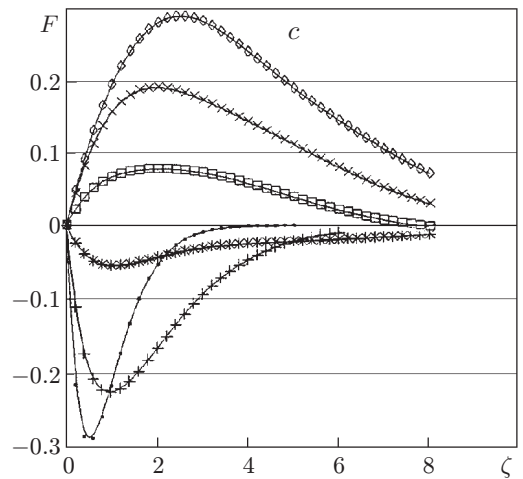
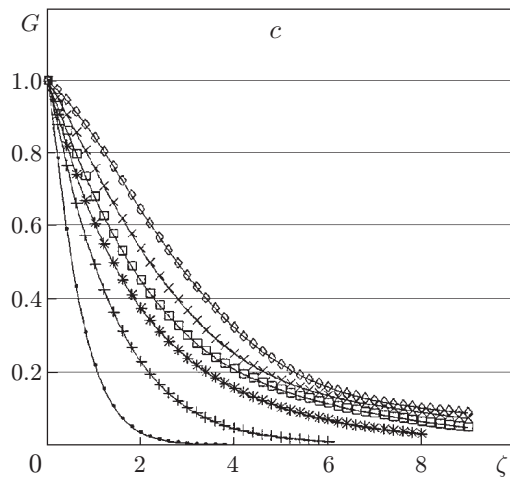
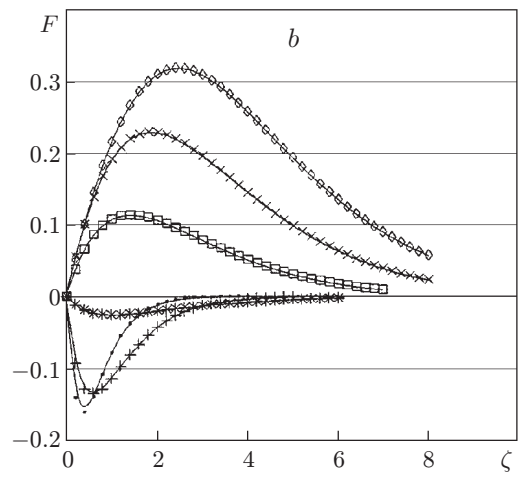
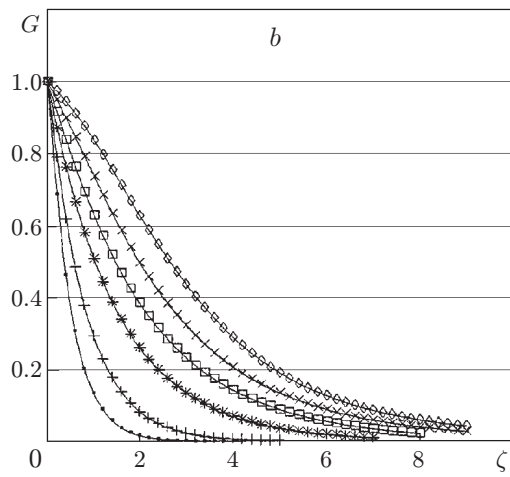
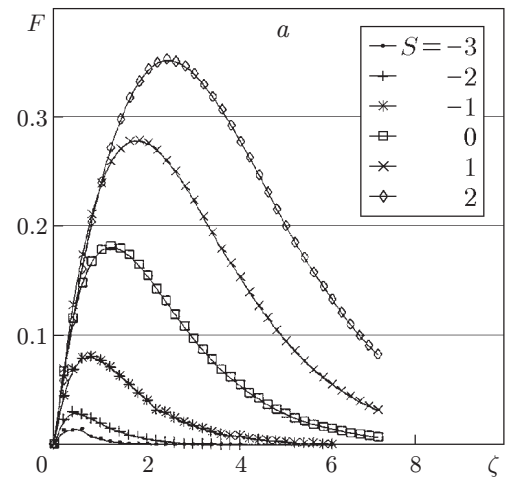
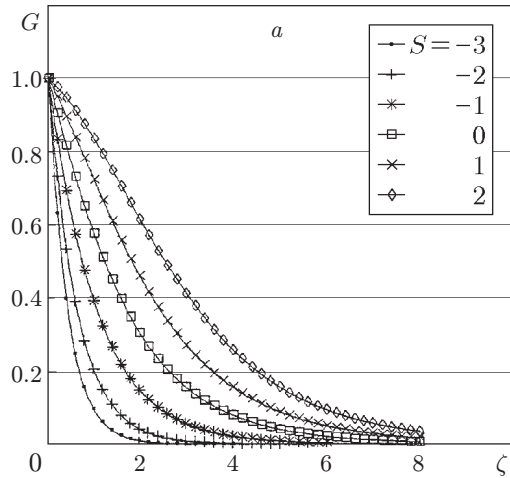


Fig. 5

Fig. 6

Fig. 5. Steady-state profiles of the parameter G for different values of S and $K = 0$ (a), 1 (b), and 2 (c).

Fig. 6. Steady-state profiles of the parameter F for different values of S and $K = 0$ (a), 1 (b), and 2 (c).

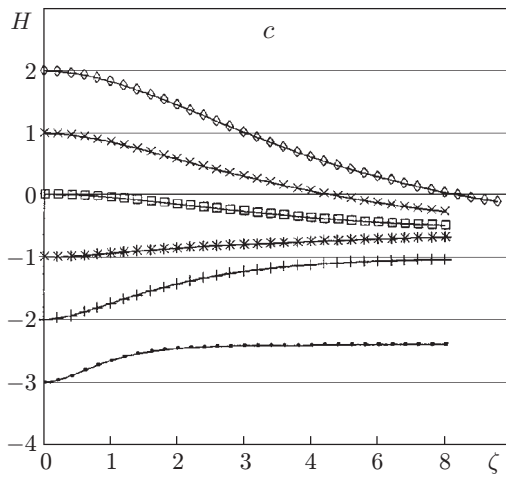
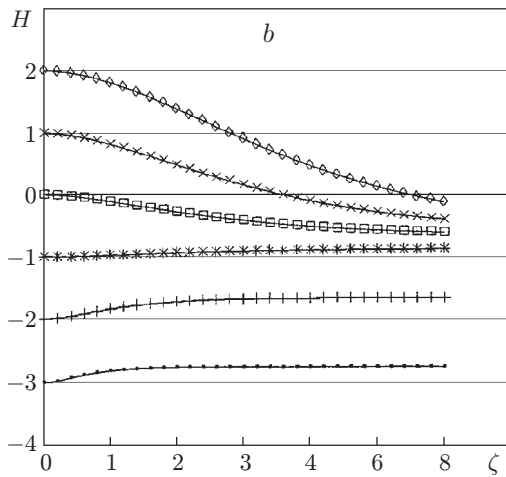
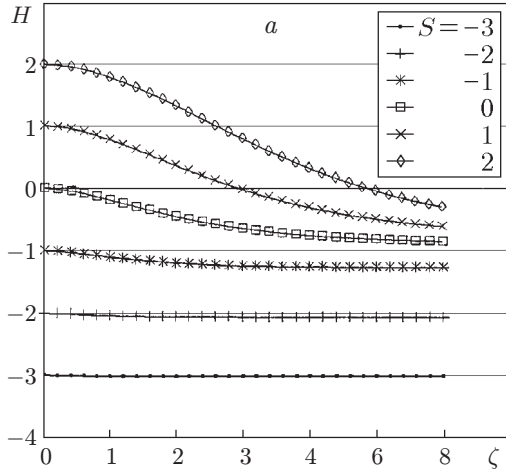


Fig. 7

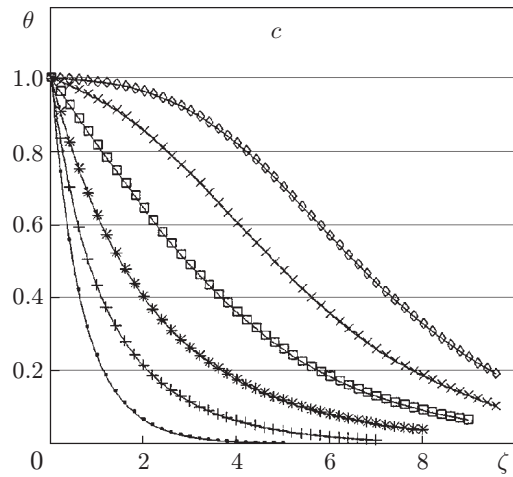
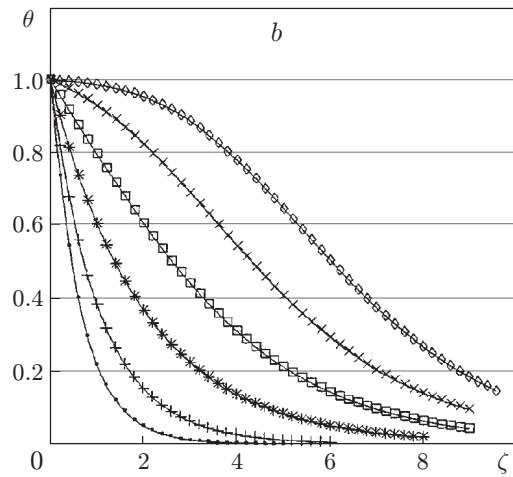
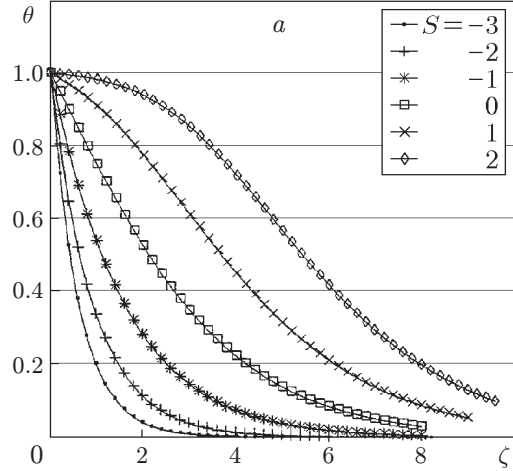


Fig. 8

Fig. 7. Steady-state profiles of the parameter H for different values of S and $K = 0$ (a), 1 (b), and 2 (c).

Fig. 8. Steady-state profiles of the parameter θ for different values of S and $K = 0$ (a), 1 (b), and 2 (c).

The results in Fig. 7 show that increasing S and K increases H for all values of ζ . For all values of K , the parameter H reverses its sign at a certain distance ζ . The values of ζ corresponding to the reversal of the sign of H increase with increasing S or K . This is caused by upward convection of the fluid by injection.

The values of θ increase with increasing S or K for all values of ζ (Fig. 8). This is caused by the influence of these parameters on the thermal resistance near the disk surface.

Conclusions. An unsteady flow of a non-Newtonian fluid with the Reiner–Rivlin viscosity model, caused by uniform rotation of an infinite porous disk, was studied in the present paper. The effect of the non-Newtonian fluid characteristics (parameter K) and suction or injection velocity (parameter S) on velocity and temperature distributions was considered. Joint examination of these parameters revealed some interesting features. It was found that the parameter K reverses the direction of axial velocity with time in the case of zero injection and even in the case of suction. It is also interesting that a change in the parameter K leads to the reversal of the direction of radial velocity $F(\zeta)$ with varied suction intensity. The non-Newtonian characteristics have a significant effect on heat transfer from the surface of the rotating disk, and this effect is more pronounced in the case of suction than in the case of injection.

REFERENCES

1. T. Von Kármán, "Über laminare und turbulente reibung," *ZAMM.*, **1**, No. 4, 233–235 (1921).
2. W. G. Cochran, "The flow due to a rotating disk," *Proc. Cambridge Philos. Soc.*, **30**, No. 3, 365–375 (1934).
3. E. R. Benton, "On the flow due to a rotating disk," *J. Fluid Mech.*, **24**, No. 4, 781–800 (1966).
4. J. T. Stuart, "On the effects of uniform suction on the steady flow due to a rotating disk," *Quart. J. Mech. Appl. Math.*, **7**, 446–457 (1954).
5. H. Ockendon, "An asymptotic solution for steady flow above an infinite rotating disk with suction," *Quart. J. Mech. Appl. Math.*, **25**, 291–301 (1972).
6. H. K. Kuiken, "The effect of normal blowing on the flow near a rotating disk of infinite extent," *J. Fluid Mech.*, **47**, No. 4, 789–798 (1971).
7. K. G. Mithal, "On the effects of uniform high suction on the steady flow of a non-Newtonian liquid due to a rotating disk," *Quart. J. Mech. Appl. Math.*, **14**, 401–410 (1961).
8. A. C. Srivastava, "Flow of non-Newtonian fluids at small Reynolds number between two infinite disks: one rotating and the other at rest," *ibid.*, pp. 353–385.
9. K. Millsaps and K. Pohlhausen, "Heat transfer by laminar flow from a rotating disk," *J. Aeronaut. Sci.*, **19**, 120–126 (1952).
10. S. Ostrach and P. R. Thornton, "Compressible flow and heat transfer about a rotating isothermal disk," NACA TN 4320 (1958).
11. E. M. Sparrow and J. L. Gregg, "Heat transfer from a rotating disk to fluids of any Prandtl number," *Trans. ASME, Ser. C, J. Heat Transfer*, 249–251 (1959).
12. E. M. Sparrow and J. L. Gregg, "Mass transfer, flow, and heat transfer about a rotating disk," *Trans. ASME, Ser. C, J. Heat Transfer*, 294–302 (1960).
13. S. E. Tadros and F. F. Erian, "Generalized laminar heat transfer from the surface of a rotating disk," *Int. J. Heat Mass Transfer*, **25**, No. 11, 1615–1660 (1982).
14. G. H. Evans and R. Greif, "Forced flow near a heated rotating disk: a similarity solution," *Fluid Mech.*, **22**, No. 5, 804–807 (1988).
15. G. Le Palec, "Numerical study of convective heat transfer over a rotating rough disk with uniform wall temperature," *Int. J. Comm., Heat Mass Transfer*, **16**, No. 1, 107–113 (1989).
16. K. Hirose, T. Yokoyama, and M. Ouchi, "Numerical study of convective heat transfer on a horizontal isothermal rotating disk," *Trans. Jpn. Soc. Mech. Eng., Part B*, **61**, 3770–3775 (1995).
17. H. A. Attia, "Transient flow of a conducting fluid with heat transfer due to an infinite rotating disk," *Int. J. Comm. Heat Mass Transfer*, **28**, No. 3, 439–448 (2001).
18. G. Astarita and G. Marrucci, *Principles of Non-Newtonian Fluid Mechanics*, McGraw-Hill, New York (1974).
19. W. F. Ames, *Numerical Methods for Partial Differential Equations*, Academic Press, New York (1977).